Kinetic Modeling of Charge-Transfer Quenching in the CP29 Minor Complex

Yuan-Chung Cheng,[†,‡] Tae Kyu Ahn,[†,‡] Thomas J. Avenson,[‡,§] Donatas Zigmantas,[†,‡] Krishna K. Niyogi,[†,§] Matteo Ballottari,[||] Roberto Bassi,[||] and Graham R. Fleming*[,†,‡]

Physical Biosciences Division, Lawrence Berkeley National Laboratory, Berkeley, California 94720; Department of Chemistry, Hildebrand B77, University of California, Berkeley, California 94720-1460; Department of Plant and Microbial Biology, 111 Koshland Hall, University of California, Berkeley, California 94720-3102; and Department of Science and Technology, University of Verona, Verona, Italy 37134

Received: March 30, 2008; Revised Manuscript Received: August 12, 2008

We performed transient absorption (TA) measurements on CP29 minor light-harvesting complexes that were reconstituted in vitro with either violaxanthin (Vio) or zeaxanthin (Zea) and demonstrate that the Zea-bound CP29 complexes exhibit charge-transfer (CT) quenching that has been correlated with the energy-dependent quenching (qE) in higher plants. Simulations of the difference TA kinetics reveal two-phase kinetics for intracomplex energy transfer to the CT quenching site in CP29 complexes, with a fast <500 fs component and a ~6 ps component. Specific chlorophyll sites within CP29 are identified as likely locations for CT quenching. We also construct a kinetic model for CT quenching during qE in an intact system that incorporates CP29 as a CT trap and show that the model is consistent with previous in vivo measurements on spinach thylakoid membranes. Finally, we compare simulations of CT quenching in thylakoids with those of the individual CP29 complexes and propose that CP29 rather than LHCII is a site of CT quenching.

1. Introduction

Higher plant photosynthesis initiates with absorption of light energy in the antenna of photosystems (PS) I and II,[1] both of which contain multiple light-harvesting complexes (LHCs).[2] The periphery of the PSII antenna is comprised of trimeric LHCII complexes which are considered the major LHCs.[3] In between the reaction center and the peripheral LHCII are three minor complexes referred to as CP24, CP26, and CP29.[4−7] These trimeric LHCII and minor complexes bind chlorophylls and carotenoids that absorb sunlight and transfer the energy to the reaction center for photosynthesis. Under conditions in which light energy is absorbed in excess of photosynthetic capacity, pigments within these LHCs are exchanged, resulting in harmless thermal dissipation of the excessively absorbed energy. This phenomenon is generally referred to as nonphotochemical quenching (NPQ). In higher plants, the predominant component of NPQ is rapidly reversible and is termed energy-dependent quenching (qE).[8,9]

qE is a complex physiological response[8−10] that depends upon (1) the buildup of a pH gradient across the thylakoid membranes (ΔpH),[11] (2) the formation of a xanthophyll species called zeaxanthin (Zea),[12,13] and (3) PsbS, a PSII antenna-associated polypeptide that has been suggested to sense changes in the pH of the thylakoid lumen and possibly cause conformational changes throughout the antenna to control qE.[14,15] All these components conspire in vivo to bring about the maximum yield of qE quenching.[16] Although the phenomenology of qE has been documented for years, a fundamental understanding of its physical mechanism remains unclear.[8,9,17]

Based initially on theoretical quantum chemical calculations, we proposed a mechanism for quenching of chlorophyll excited states during qE involving charge transfer (CT) within a chlorophyll−zeaxanthin (Chl−Zea) heterodimer.[18,19] This mechanism predicts that dissipation of chlorophyll excited states will be accompanied by transient zeaxanthin radical cation ($Zea^{\bullet+}$) formation. We performed ultrafast transient absorption (TA) experiments on isolated thylakoids by exciting the chlorophyll Q_y transition and probing for transient species in the near-infrared region (NIR). The NIR TA kinetic for light-adapted thylakoids indicated transient $Zea^{\bullet+}$ formation in a qE-dependent manner.[20] These results clearly demonstrate that CT quenching is a physical mechanism specific for qE and that zeaxanthin (Zea) is directly involved in CT quenching during qE.[20] However, they do not provide information regarding the location of Chl−Zea CT quenching sites in LHCs.

To reveal which of the LHCs in the PSII antenna mediate CT quenching and achieve a molecular-level understanding of NPQ, we have investigated isolated LHCs separately. We observed evidence for transient $Zea^{\bullet+}$ formation in a composite mixture of isolated monomeric LHCs (i.e., monomeric LHCII, CP24, CP26, and CP29) and also showed that the transient $Zea^{\bullet+}$ signal could not be detected in LHCII monomers reconstituted in vitro with either violaxanthin (Vio) or Zea.[21] Therefore, the $Zea^{\bullet+}$ signal observed in the mixture of monomers arose solely within one or more minor complexes that bind Zea. These results suggest that minor complexes contain the site(s) of CT quenching. To locate specific sites of CT quenching, we carried out NIR TA measurements on isolated minor complexes and a series of CP29 mutants.[22] Through a combination of molecular genetics and femtosecond spectroscopy, we demonstrate CT quenching in all three of the individual minor complexes and that CT quenching in CP29 involves a specific pair of excitonically coupled chlorophylls acting as the electron acceptor.[22] We proposed that an equilibrium exists between nonquenching (N) and quenching (Q) forms: LHC(N) ↔ LHC(Q). The equilibrium

* To whom correspondence should be addressed. E-mail GRFleming@lbl.gov. Tel: 510-643-2735. Fax: 510-643-6340.
[†] Lawrence Berkeley National Laboratory.
[‡] Department of Chemistry, UC, Berkeley.
[§] Department of Plant and Microbial Biology, UC, Berkeley.
[||] University of Verona.

10.1021/jp802730c CCC: $40.75
Published on Web 09/30/2008

is most likely modulated in vivo by contributions from Zea, PsbS, and the transthylakoid ΔpH to regulate qE. In addition, although maximum qE, and therefore maximum CT quenching, is dependent upon an intact system, the minor complexes can attain the quenching conformation in vitro when Zea is bound to it. We estimated that less than 1% of the isolated minor complexes were engaged in CT quenching in vitro, whereas between 40 and 80% of the minor complexes were estimated to be active in CT quenching in thylakoids engaged in steady-state qE in vivo. At this fraction, CT quenching can account for the magnitude of qE observed in vivo.[21] Therefore, results of our previous in vivo[20] and in vitro[21,22] measurements are consistent and suggest that CT quenching in minor complexes is a critical mechanism for qE.

In this work, we aim to provide a basic kinetic model for excitation quenching in the PSII antenna and assess whether the $Zea^{\bullet+}$ signature of CT quenching in an individual minor complex can be modeled consistently. We studied CP29 minor complexes that were reconstituted in vitro with chlorophylls (*a* and *b*) and either Vio or Zea and probe for evidence of $Zea^{\bullet+}$ formation in the Zea-bound CP29 complexes. We also construct a kinetic model for CT quenching in an intact system (in which LHCII participates in energy transfer dynamics) that incorporates a minor complex as a CT trap and perform simulations of the difference NIR TA kinetics based on this model. The simulations provide insight into energy transfer dynamics within trapping CP29 complexes and provide support for a model based on minor complexes as the sites of CT quenching in PSII at high light levels.

2. Materials and Methods

2.1. CP29 Sample Preparation. The gene for CP29 was expressed in *E. coli*, and the apoprotein was isolated, followed by in vitro reconstitution with chlorophylls (*a* and *b*), lutein, and either Vio or Zea.[23] For NIR TA kinetic analyses, the CP29 complexes were resuspended in buffer solution (5 mM HEPES and 0.06% α-DM at pH 7.6) to an optical density of ∼0.3/mm.

2.2. NIR TA Measurements. The NIR TA laser system has been described previously.[20] The repetition rate was 250 kHz, and the pump pulses were tuned to ∼650 nm (i.e., the chlorophyll *b* Q_y transition). The maximum pump energy and fwhm of the pulse autocorrelation trace were 48 nJ/pulse and ∼40 fs, respectively. White light continuum probe pulses were generated in a 1 mm quartz plate. The observation of the cross-correlation function of the pump and probe overlap was ca. 85 fs. The mutual polarizations of the pump and probe beams were set to the magic angle (54.7°). The time resolution of our TA measurements was 5 ps/point (−60 to −10 ps), 0.5 ps/point (−10 to 60 ps), and 5 ps/point (65 to 600 ps). A monochromator (Spectra Pro 300i, Acton Research Corp., Acton, MA) with a spectral resolution of 2.7 nm and a InGaAs photodiode (DET410, Thorlabs, Newton, NJ) was used to monitor transmission. A sample cell with a path length of 1 mm was chilled by a circulating water bath (VWR Scientific 1160, PolyScientific, Niles, IL) which was set at 7 °C during the data acquisition to prevent sample degradation.

2.3. Kinetics Modeling. In this study, the mechanism of CT quenching in PSII is described by the four-state model presented in Figure 1, which is an extension of the three-state model used by Holt et al.[20] This model includes energy transfer from bulk chlorophylls to an intermediate chlorophyll in minor complexes, assuming the minor complexes are the sites of CT quenching during qE as has been suggested.[21,22] The differential equations that describe the time evolution

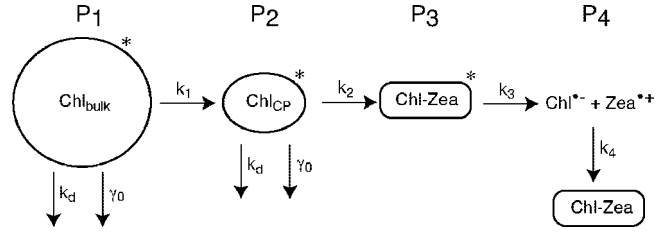

Figure 1. Model for the charge-transfer quenching mechanism of qE in the photosystem II supercomplex. Assuming the minor complexes are the site of CT quenching, four species are required for the description of CT quenching after selective excitation of the Chl Q_y excited states: the Q_y excited state on a chlorophyll molecule in bulk LHCs (Chl^*_{bulk}, predominantly on LHCII), the Q_y excited state on a chlorophyll molecule in the minor complexes (Chl^*_{CP}), the excited Chl−Zea heterodimer [(Chl−Zea)*], and the charge-separated state ($Chl^{\bullet-}-Zea^{\bullet+}$). They are described by normalized populations P_1, P_2, P_3, and P_4, respectively.

of populations after selective excitation of the chlorophyll Q_y band are

$$\frac{dP_1}{dt} = -k_1P_1 - k_dP_1 - \frac{1}{2}\gamma_0P_1^2 \quad (1)$$

where P_1, P_2, P_3, and P_4 are the normalized populations of

$$\frac{dP_2}{dt} = k_1P_1 - k_2P_2 - k_dP_2 - \frac{1}{2}\gamma_0P_2^2 \quad (2)$$

$$\frac{dP_3}{dt} = k_2P_2 - k_3P_3 \quad (3)$$

$$\frac{dP_4}{dt} = k_3P_3 - k_4P_4 \quad (4)$$

the bulk chlorophyll excited state (Chl^*_{bulk}), the excited state on a chlorophyll in a minor complex (Chl^*_{CP}), the excited Chl−Zea heterodimer [(Chl−Zea)*], and the charge-separated state ($Chl^{\bullet-}-Zea^{\bullet+}$), respectively. To obtain a description that is not explicitly dependent on the intensity of the laser pulses, we scale all populations by the initial excited-state population on all chlorophylls so that $P_1 + P_2 + P_3 = 1$ at time zero.[24,25] This model describes the intercomplex energy transfer from excited bulk Chl to the minor complex (k_1), the intracomplex energy transfer within the minor complexes to the quencher heterodimer (k_2), the generation of charge-separated state (k_3), and the recombination of the charges to recover the heterodimer ground state (k_4). Moreover, additional de-excitation contribution (k_d) and excited chlorophyll singlet−singlet annihilation (γ_0) are also considered.

A simple kinetic model described by a second-order rate constant γ_0 is included to describe singlet−singlet annihilation of chlorophyll excited states. With the normalized population description, γ_0 is defined as the true second-order singlet−singlet annihilation rate times the initial excited-state population on all chlorophylls. In principle, such a kinetic approach is only applicable to large aggregates,[24,25] and γ_0 should depend on the size of the antenna. We neglect these details of the singlet−singlet annihilation dynamics in the present study because in our modeling of the experimental difference kinetic data, the chlorophyll excited-state population is not directly fitted to the measurements, and the simple kinetic model for annihilation seems to give a reasonable description for the experimental

results. Therefore, the interpretation of the values of γ_0 extracted from fitting to the difference kinetics here should be taken with care. To accurately model the annihilation dynamics, the initial distribution of chlorophyll excitations in the ensemble of complexes has to be considered,[25] and the ESA contribution has to be treated explicitly by modeling the absolute NIR TA kinetics (instead of the difference kinetics modeled here), which is beyond the scope of this work.

Furthermore, the additional ultrafast (<500 fs) energy transfer dynamics within the minor complexes is not included explicitly. Instead, it is considered using nonzero population on the heterodimer site as if the heterodimers are directly excited, effectively coarse graining all the neighboring sites that transfer energy rapidly to the heterodimer sites as precursors to the $Chl^{\bullet-}-Zea^{\bullet+}$ charge-separated state. In our modeling, we found that the population dynamics of the $Chl^{\bullet-}-Zea^{\bullet+}$ species is rather insensitive to the value of k_d when $k_1, k_2 \gg k_d$. Therefore, k_d is set to 1 ns in all our simulations. In addition, we neglected the energy transfer from the minor complex back to the bulk chlorophyll excited states in this work. In our fits to the measurement using thylakoid membranes,[20] we found that $k_2, k_3 \gg k_1$. As a result, simulations including the back transfer do not provide noticeable improvement to the fit to the experimental difference TA kinetic. The back transfer can be easily added to the simulation when it is necessary.

Our data analysis is based on the NIR TA difference profile obtained by subtracting the TA kinetics of the Vio-bound CP29 complex from those of the Zea-bound CP29 sample. We assume that the chlorophyll ESA dynamics (predominantly singlet−singlet annihilation) contribute equally to the NIR TA signals of Vio-bound and Zea-bound complexes at the same sample OD and laser intensity and attribute the observed difference kinetics directly to the population of the charge-separated states ($Chl^{\bullet-}-Zea^{\bullet+}$).[20−22] Equations 1−4 were solved numerically using a fourth-order Runge−Kutta method[26] to obtain the normalized cation population P_4 at varied rate constants. In addition, a least-squares routine is used to fit the simulation results to the experimental difference kinetics and obtain the optimal rate constants that describe the measurements.

3. Results and Discussion

To study the dynamics of CT quenching in isolated CP29, we performed TA measurements on CP29 apoproteins reconstituted with either Vio (CP29-Vio) or Zea (CP29-Zea) upon excitation at 650 nm followed by the probing of transient species within the NIR. Figure 2 shows the NIR TA profiles for the respective complexes probed at 980 nm. The TA profile for the CP29−Vio complexes (blue trace) is characterized solely by decay features that are attributable to the dynamics of chlorophyll excited-state absorption (ESA).[20] In contrast, the TA profile for the CP29−Zea complexes (red trace) exhibits an additional ultrafast rise component followed by multiexponential decay. These results show transient carotenoid radical cation ($Car^{\bullet+}$) formation solely within the quenching CP29−Zea complexes. To determine more specifically whether this transient species is a $Zea^{\bullet+}$, we reconstructed a transient spectrum (Figure 3) using TA difference profiles (Figure 4). The spectrum shows a single peak centered at ~980 nm, in excellent agreement with the spectrum of the $Zea^{\bullet+}$ species in a protein environment established by our group recently.[20,21] Evidently, the TA profile for the CP29−Zea complexes shows the transient formation of a $Zea^{\bullet+}$ species upon selective excitation of the complexes at the chlorophyll Q_y transition. Note that the small fraction of quenching CP29−Zea complexes in our reconstituted sample

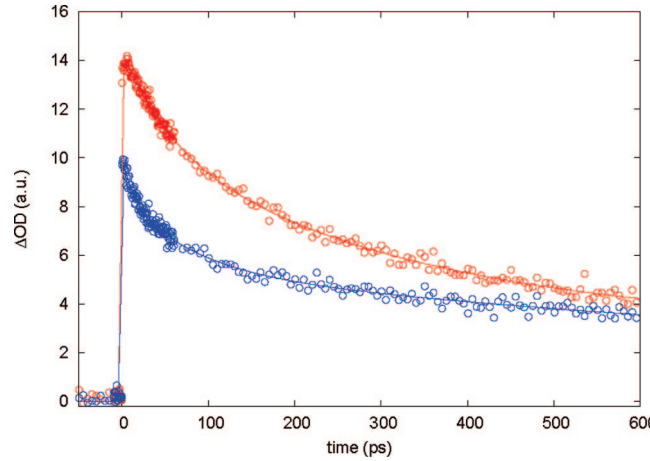

Figure 2. NIR TA kinetics for the isolated CP29 minor complexes. The TA kinetics were obtained using CP29 apoproteins reconstituted in vitro with chlorophylls (*a* and *b*) and either Vio (blue) or Zea (red). Experiments were carried out by excitation of the complexes at 650 nm and probing at 980 nm. Each trace is an average of more than 10 kinetic sweeps. The traces were not normalized in any way. Equal sample OD and excitation laser intensity were used to allow for direct comparison of the TA kinetics.

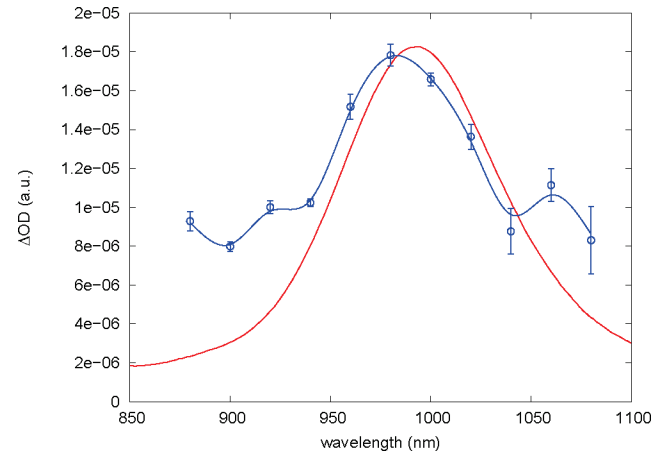

Figure 3. Reconstructed NIR spectrum for the $Zea^{\bullet+}$ species. A series of NIR TA kinetic profiles were reconstructed in CP29 complexes that bind either Vio or Zea by exciting at 650 nm and probing from 880 to 1080 nm. NIR TA difference kinetics were obtained by subtracting the TA profiles obtained using CP29 that binds Vio from those of the CP29 complexes that bind Zea. The spectrum (blue) was reconstructed by estimating the maximum amplitude of the difference profiles (i.e., average of time points 13−17 ps) at ~15 ps. Error bars represent the standard error of the mean of 5 time points. Shown for comparison is the solution spectrum of the β-carotene radical cation (red) from ref 27.

(~1%) can still give rise to a significant NIR TA signal without being overwhelmed by the chlorophyll ESA, because (1) the singlet−singlet annihilation process removes chlorophyll excited-state population rapidly and (2) the absorption cross section of carotenoid cation is more than an order of magnitude higher than that of the chlorophyll excited state in the NIR regime.[21,27,28] Finally, NIR TA measurements on two other minor complexes (CP24 and CP26) were also performed, and similar results were obtained (data not shown). These data are consistent with our previous study showing that minor complexes are likely to be responsible for CT quenching in PSII during engagement of qE.[21,22]

Analysis based on the absorption cross section of chlorophyll and our pump laser intensity[21] suggests that a chlorophyll has ~30% probability to be excited in the CP29 experiment. Given

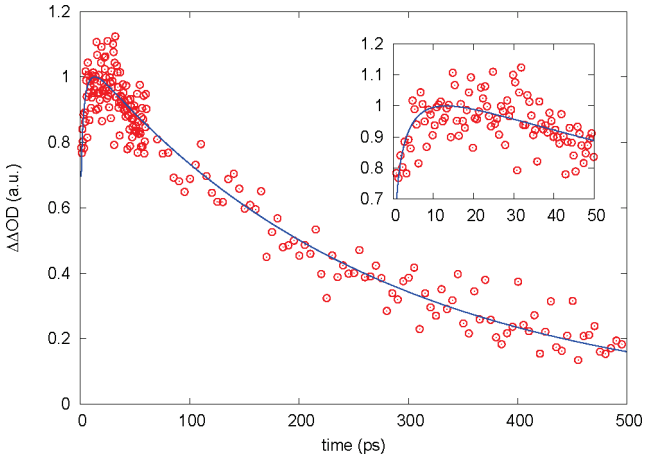

Figure 4. NIR difference TA kinetics for the isolated CP29 minor complex. The measurements (circles) and theoretical fit based on the charge-transfer quenching model (blue line) are shown. The parameters for the theoretical fit are $\tau_2 \sim 6$ ps, $\tau_3 = 0.1-0.3$ ps, $\tau_4 = 260$ ps, and $1/\gamma_0 \sim 0.1$ ps.

that ~4 Chls in each CP29 complex absorb at the excitation wavelength (650 nm), a significant portion of the excited CP29 complexes in the experiment is doubly excited. Therefore, a strong singlet−singlet annihilation contribution is expected in the experiment. Power-dependent measurements on the same sample also indicate a significant annihilation contribution to the Chl ESA dynamics at this laser intensity (data not shown). Detailed analysis of power-dependent data based on a more sophisticated model for annihilation is currently in progress and will be published elsewhere.

The difference between the TA traces for the CP29−Vio and CP29−Zea complexes approaches zero at long times, implying that the ESA dynamics (predominantly singlet−singlet annihilation) contribute equally in both complexes.[20−22] Assuming the ESA dynamics of the CP29−Zea (quenched) and CP29−Vio (unquenched) complexes contribute equally to the NIR TA signals, the difference TA kinetic represents the dynamics of $Zea^{\bullet+}$ formation. Therefore, we focus on the difference TA kinetic profile obtained by subtracting the TA kinetics of the CP29−Vio complex from those of the CP29−Zea. The difference TA kinetic shown in Figure 4 indeed demonstrates the formation and decay of $Zea^{\bullet+}$, consistent with the transfer of energy from singlet excited chlorophyll to a Chl−Zea heterodimer that undergoes rapid charge separation followed by charge recombination (Figure 1). In addition, the rise of the signal clearly exhibits biphasic behavior: a fast <500 fs component gives rise to the nonzero difference transient absorption ($Zea^{\bullet+}$ population) at $t \sim 0$ and a slower component that results in the later increase of the difference signal. The ultrafast component can be attributed to either direct excitation of the Chl−Zea heterodimer or rapid energy transfer from excited chlorophylls to the heterodimer site, neither of which are distinguishable because the time resolution of the current data set is not sufficient to show subpicosecond energy transfer steps. Note that the excitation wavelength in the current experiment is 650 nm, which is on the blue side of the CP29 Q_y absorption band. Since the heterodimer quenching species should absorb at the red side of the band, it is unlikely that a significant portion of the heterodimers are directly excited during the experiment. Therefore, the <500 fs formation of the $Zea^{\bullet+}$ species is more likely due to ultrafast energy transfer to the heterodimer. Nevertheless, because of the limited time resolution in the experimental data, we did not explicitly include the ultrafast (<500 fs) energy transfer dynamics within the minor complexes in our kinetic modeling. Instead, nonzero initial population on the heterodimer excited state was considered, effectively coarse-graining all the neighboring sites that transfer energy rapidly to the heterodimer site as precursors to the $Chl^{\bullet-}-Zea^{\bullet+}$ charge-separated state.

To describe the CP29 data, we used the kinetics model described in Figure 1 (without the Chl^*_{bulk} block, $P_1 = 0$) to fit the population of the $Zea^{\bullet+}$ species (P_4) with nonzero initial population on the heterodimer excited state (P_3) and found that an initial population $P_3 > 0.2$ is required to fit the difference kinetics at short times. The modeling also shows that the TA data are best described by $\tau_2 = 1/k_2 \sim 6$ ps, $\tau_3 = 1/k_3 = 0.1-0.3$ ps, $\tau_4 = 1/k_4 = 260$ ps, and $1/\gamma_0 = 0.13$ ps (Figure 4). Energy relaxation into the CT quenching site at longer time scales may exist but cannot be resolved in the rise component of our experiment. The modeling indicates that a significant portion of the Chl−Zea heterodimers that underwent CT quenching are either directly excited or rapidly accept excitation from neighboring chromophores on a <500 fs time scale. Additional quenching happens on a time scale of 6 ps, which we attribute to slower intracomplex energy transfer within a CP29 complex. In fact, such biphasic energy transfer dynamics are in excellent agreement with previous studies of excitation energy transfer in LHCII and CP29 complexes.[29−37] In particular, Holzwarth and co-workers studied excitation energy transfer in isolated CP29 complexes using ultrafast pump−probe spectroscopy and theoretical calculations based on the Forster theory, and they also observed general multiexponential dynamics in this system upon excitation at 650 nm.[29,31,30] Moreover, they were able to produce a map of energy transfer pathways in the CP29 complex and assign the ultrafast component to energy transfer within blocks of strongly coupled chlorophylls and the slower component to energy transfer between chlorophyll blocks.[29] According to their block diagram of CP29 energy transfer pathways, only the block containing chlorophyll A1 and A2 and the block containing chlorophyll A4, A5, and B5 (labeled using the convention in refs29, 38, and 39) exhibit an intrablock energy transfer time scale of <500 fs and an interblock transfer time scale of ~6 ps.[40] Therefore, our observations, together with the block diagram of energy transfer pathways in CP29 suggested by Holzwarth and co-workers, indicate that the Chl−Zea heterodimer site might be comprised of any of the chlorophylls A1, A2, A4, A5, and B5, assuming that the energy transfer dynamics are not significantly affected by the activation of CT quenching in Zea-bound CP29 complexes. Chlorophylls A1 and A2, however, are not close to the Zea binding site in CP29; instead, they are both close to a lutein molecule.[39] In contrast, chlorophylls A4, A5, and B5 are close to the Zea binding site in CP29[41] and are more likely to be in position to form a Chl−Zea CT quenching heterodimer upon exchange of xanthophylls. Note that there are already several pieces of evidence indicating that the A5 and B5 pair is a critical site of regulation in LHC proteins,[22,42,43] which is consistent with the data and kinetic modeling presented in this work. In particular, we have applied the NIR TA technique in an independent study to a series of mutant CP29 complexes that each lacked a specific Chl, and the results also strongly support the idea that both A5 and B5 Chls are essential for CT quenching; i.e., the architecture of the CT quenching site in CP29 consists of a pair of coupled Chls (A5 and B5) and a Zea molecule.[22] All together, we suggest that chlorophylls A5 and B5 are the best candidates for the CT quenching site.

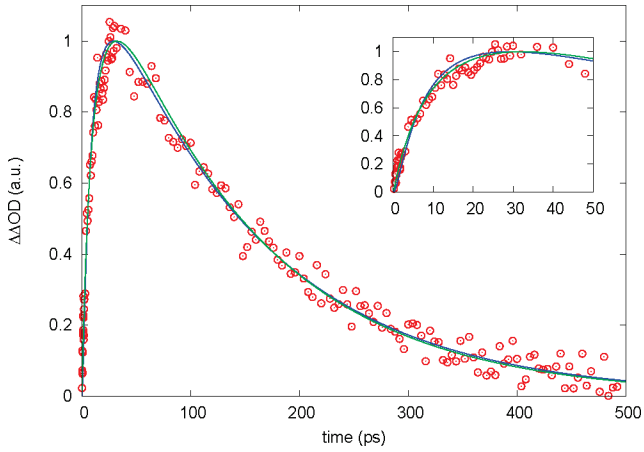

Figure 5. NIR difference TA kinetics for the thylakoid sample in vivo measured in our previous work.[20] The measurements (circles) and theoretical fit based on the charge-transfer quenching model with (blue line) and without (green line) a minor complex intermediate state are shown. The parameters for the theoretical fit with a minor complex intermediate state are $\tau_1 \sim 20$ ps, $\tau_2 \sim 6$ ps, $\tau_3 = 0.1-0.3$ ps, $\tau_4 = 145$ ps, and $1/\gamma_0 = 0.1$ ps. The three-state and four-state models are indistinguishable.

Finally, in order to examine whether the minor complex quenching model (Figure 1) is consistent with observations of qE in vivo, we also modeled the dynamics of $Zea^{\bullet+}$ formation in spinach thylakoid membranes[20] using the four-state model described in Figure 1, i.e., with an additional minor complex intermediate state. We found that the data are well described by the four-state model using $\tau_1 = 1/k_1 \sim 20$ ps, $\tau_2 \sim 6$ ps, $\tau_3 = 0.1-0.3$ ps, $\tau_4 = 145$ ps, and $1/\gamma_0 = 0.1$ ps (Figure 5). Our experimental data cannot distinguish the four-state model from the three-state model used in ref 20. However, both models indicate that the averaged energy transfer time scale from bulk chlorophylls to the CT quenching site is ~20 ps, which is significantly longer than the intracomplex transfer time of ~6 ps observed in the CP29 CT quenching. We assign the longer time scale for $Zea^{\bullet+}$ formation in the thylakoid membranes to intercomplex energy transfer, most likely from LHCII to a CT quenching site in the minor complexes. The time scale agrees well with the time scale of energy equilibration in aggregates of LHCII complexes.[25] Notably, the lack of <5 ps rapid rise component in the $Zea^{\bullet+}$ signal in spinach thylakoid membranes implies that the CT quenching the Chl−Zea heterodimer is not located inside the LHCII complex; otherwise, CT quenching within LHCII (which should account for the bulk of chlorophyll excited states according to chlorophyll ratios in comparison to minor complexes) would be expected to give rise to rapid formation of the $Zea^{\bullet+}$ species due to fast <5 ps energy equilibration within LHCII complexes.[34,33,36,37] Therefore, on the basis of kinetic modeling, we suggest that the thylakoid $Zea^{\bullet+}$ formation kinetics correspond primarily to energy transfer from LHCII to trap sites within the minor complexes.

4. Conclusions

We proposed in a previous work that the minor complexes are sites of CT quenching during qE.[21] The present study on isolated Zea-bound CP29 complexes enables dissection of the components that are responsible for qE and provides strong support for the minor complex CT quenching model. We have shown that the dynamics of $Zea^{\bullet+}$ formation in isolated CP29 complexes could be well described by intracomplex energy transfer to a Chl−Zea heterodimer within the minor complex, which then undergoes rapid charge separation to form $Zea^{\bullet+}$ (Figure 1). In addition, our kinetic modeling demonstrates that energy transfer to the heterodimer quenching site is biphasic, with a fast <500 fs component that corresponds to energy transfer within blocks of strongly coupled chlorophylls to the quenching heterodimer and a slower ~6 ps component that corresponds to interblock energy transfer within the CP29 complex. These time scales are in excellent agreement with previous ultrafast studies and, when combined with the block diagram of energy transfer pathways in CP29,[29,31] indicate that the CT quenching heterodimer is likely to involve at least one of the A1, A2, A4, A5, and B5 sites in CP29. Further consideration based on the proximity to the Zea binding site[44,43] for these chlorophylls suggests that sites A4, A5, and B5 are more likely to be involved in CT quenching. This result is in excellent agreement with our recent experiments in which the individual chlorophyll molecules are successively removed from the CP29 complex.[22] Combining these experimental observations, we suggest that the architecture of the CT quanching site in CP29 consists of a pair of coupled Chls (A5 and B5) and a Zea molecule, which form the molecular basis of CT quenching during qE.

We also modeled the dynamics of $Zea^{\bullet+}$ formation in spinach thylakoid membranes using the minor complex CT quenching model (Figure 1) and showed that the model is consistent with the measurements in vivo. A fit to the thylakoid data showed that the time scale of energy transfer to the heterodimer quenching site is ~20 ps, in contrast to the ~6 ps intracomplex transfer rate observed in isolated CP29 complex. The finding that no <6 ps rise component is observed in the dynamics of $Zea^{\bullet+}$ formation in spinach thylakoid membranes supports the notion that the CT quenching site is not within the LHCII trimer complex. We therefore conclude that the model presented in Figure 1, in which the minor complexes are identified as the sites of CT quenching, provides a basic molecular framework for CT quenching during qE.

Acknowledgment. This work was supported by the Director, Office of Science, Office of Basic Energy Sciences, of the U.S. Department of Energy under Contract DE-AC02-05CH11231 and by the Chemical Sciences, Geosciences and Biosciences Division, Office of Basic Energy Sciences, U.S. Department of Energy, under Contract DE-AC03-76SF000098 (G.R.F. and K.K.N), the Korea Research Foundation Grant (KRF-2006-214-C00037) funded by the Korean Government (MOEHRD) (T.K.A.), and the National Research Initiative Competitive Grant (2006-03279) (T.J.A.). R.B. extends thanks to the FIRB Contract RBLA0345SF from the Italian Basic Research Foundation and contract SAMBA Trento Research Council for foundational support.

References and Notes

(1) Dekker, J. P.; Boekema, E. J. *Biochim. Biophys. Acta* **2005**, *1706*, 12–39.
(2) Green, B.; Durnford, D. *Annu. Rev. Plant Physiol. Plant Mol. Biol.* **1996**, *47*, 685–714.
(3) Formaggio, E.; Cinque, G.; Bassi, R. *J. Mol. Biol.* **2001**, *314*, 1157–66.
(4) Dainese, P.; Bassi, R. *J. Biol. Chem.* **1991**, *266*, 8136–42.
(5) Harrer, R.; Bassi, R.; Testi, M. G.; Schäfer, C. *Eur. J. Biochem.* **1998**, *255*, 196–205.
(6) Boekema, E. J.; Hankamer, B.; Bald, D.; Kruip, J.; Nield, J.; Boonstra, A. F.; Barber, J.; Rögner, M. *Proc. Natl. Acad. Sci. U.S.A.* **1995**, *92*, 175–9.
(7) Boekema, E. J.; van Roon, H.; Calkoen, F.; Bassi, R.; Dekker, J. P. *Biochemistry* **1999**, *38*, 2233–9.
(8) Horton, P.; Ruban, A. V.; Walters, R. *Annu. Rev. Plant Physiol. Plant Mol. Biol.* **1996**, *47*, 655–684.

(9) Müller, P.; Li, X.-P.; Niyogi, K. K. *Plant Physiol.* **2001**, *125*, 1558–66.
(10) Kramer, D. M.; Avenson, T. J.; Edwards, G. E. *Trends Plant Sci.* **2004**, *9*, 349–57.
(11) Briantais, J. M.; Vernotte, C.; Picaud, M.; Krause, G. H. *Biochim. Biophys. Acta* **1979**, *548*, 128–38.
(12) Niyogi, K. K.; Grossman, A. R.; Björkman, O. *Plant Cell* **1998**, *10*, 1121–34.
(13) Demmig-Adams, B. *Biochim. Biophys. Acta* **1990**, *1020*, 1–24.
(14) Li, X.-P.; Björkman, O.; Shih, C.; Grossman, A. R.; Rosenquist, M.; Jansson, S.; Niyogi, K. K. *Nature (London)* **2000**, *403*, 391–5.
(15) Li, X.-P.; Gilmore, A. M.; Caffarri, S.; Bassi, R.; Golan, T.; Kramer, D. M.; Niyogi, K. K. *J. Biol. Chem.* **2004**, *279*, 22866–74.
(16) Niyogi, K. K.; Li, X.-P.; Rosenberg, V.; Jung, H.-S. *J. Exp. Bot.* **2005**, *56*, 375–82.
(17) Horton, P.; Wentworth, M.; Ruban, A. *FEBS Lett.* **2005**, *579*, 4201–6.
(18) Dreuw, A.; Fleming, G. R.; Head-Gordon, M. *Phys. Chem. Chem. Phys.* **2003**, *5*, 3247–3256.
(19) Dreuw, A.; Fleming, G. R.; Head-Gordon, M. *Biochem. Soc. Trans.* **2005**, *33*, 858–62.
(20) Holt, N. E.; Zigmantas, D.; Valkunas, L.; Li, X.-P.; Niyogi, K. K.; Fleming, G. R. *Science* **2005**, *307*, 433–6.
(21) Avenson, T. J.; Ahn, T. K.; Zigmantas, D.; Niyogi, K. K.; Li, Z.; Ballottari, M.; Bassi, R.; Fleming, G. R. *J. Biol. Chem.* **2007**, *283*, 3550.
(22) Ahn, T. K.; Avenson, T. J.; Ballottari, M.; Cheng, Y.-C.; Niyogi, K. K.; Bassi, R.; Fleming, G. R. *Science* **2008**, *320*, 794.
(23) Giuffra, E.; Cugini, D.; Croce, R.; Bassi, R. *Eur. J. Biochem.* **1996**, *238*, 112–20.
(24) Valkunas, L.; Trinkunas, G.; Liuolia, V.; van Grondelle, R. *Biophys. J.* **1995**, *69*, 1117–29.
(25) Barzda, V.; Gulbinas, V.; Kananavicius, R.; Cervinskas, V.; van Amerongen, H.; van Grondelle, R.; Valkunas, L. *Biophys. J.* **2001**, *80*, 2409–21.
(26) Press, W. H.; Flannery, B. P.; Teukolsky, S. A.; Vetterling, W. T. *Numerical Recipes in C: The Art of Scientific Computing*; Cambridge University Press: New York, 1992.
(27) Tracewell, C. A.; Brudvig, G. W. *Biochemistry* **2003**, *42*, 9127–36.
(28) Han, R.-M.; Tian, Y.-X.; Wu, Y.-S.; Wang, P.; Ai, X.-C.; Zhang, J.-P.; Skibsted, L. H. *Photochem. Photobiol.* **2006**, *82*, 538.
(29) Cinque, G.; Croce, R.; Holzwarth, A. R.; Bassi, R. *Biophys. J.* **2000**, *79*, 1706.
(30) Croce, R.; Müller, M. G.; Bassi, R.; Holzwarth, A. R. *Biophys. J.* **2003**, *84*, 2508–16.
(31) Croce, R.; Müller, M. G.; Caffarri, S.; Bassi, R.; Holzwarth, A. R. *Biophys. J.* **2003**, *84*, 2517–32.
(32) Gradinaru, C. C.; Pascal, A. A.; van Mourik, F, F.; Robert, B.; Horton, P.; van Grondelle, R.; van Amerongen, H. *Biochemistry.* **1998**, *37*, 1143–9.
(33) Salverda, J. M.; Vengris, M.; Krueger, B. P.; Scholes, G. D.; Czarnoleski, A. R.; Novoderezhkin, V. I.; van Amerongen, H.; van Grondelle, R. *Biophys. J.* **2003**, *84*, 450–65.
(34) Agarwal, R.; Krueger, B. P.; Scholes, G. D.; Yang, M.; Yom, J.; Mets, L.; Fleming, G. R. *J. Phys. Chem. B* **2000**, *104*, 2908–2918.
(35) Novoderezhkin, V. I.; Palacios, M. A.; van Amerongen, H.; van Grondelle, R. *J. Phys. Chem. B* **2004**, *108*, 10363–10375.
(36) Novoderezhkin, V. I.; Palacios, M. A.; van Amerongen, H.; van Grondelle, R. *J. Phys. Chem. B* **2005**, *109*, 10493–504.
(37) Linnanto, J.; Martiskainen, J.; Lehtovuori, V.; Ihalainen, J. A.; Kananavicius, R.; Barbato, R.; Korppi-Tommola, J. *Photosynth. Res.* **2006**, *87*, 267–79.
(38) Kühlbrandt, W.; Wang, D. N.; Fujiyoshi, Y. *Nature (London)* **1994**, *367*, 614–21.
(39) Bassi, R.; Croce, R.; Cugini, D.; Sandonà, D. *Proc. Natl. Acad. Sci. U.S.A.* **1999**, *96*, 10056–61.
(40) We note that the B5 site in CP29 is considered to be a mixed site that binds both Chls *a* and *b* (see ref 39). Therefore, when a Chl *a* is bound to the B5 site, it is capable of being the CT quenching site.
(41) Morosinotto, T.; Castelletti, S.; Breton, J.; Bassi, R.; Croce, R. *J. Biol. Chem.* **2002**, *277*, 36253.
(42) Morosinotto, T.; Breton, J.; Bassi, R.; Croce, R. *J. Biol. Chem.* **2003**, *278*, 49223.
(43) Croce, R.; Mozzo, M.; Morosinotto, T.; Romeo, A.; Hienerwadel, R.; Bassi, R. *Biochemistry* **2007**, *46*, 3846–61.
(44) Liu, Z.; Yan, H.; Wang, K.; Kuang, T.; Zhang, J.; Gui, L.; An, X.; Chang, W. *Nature (London)* **2004**, *428*, 287–92.

JP802730C